

**EVOLUTION OF PEAKS  
IN WEAKLY NONLINEAR DENSITY FIELD  
AND DARK HALO PROFILES**

EWA L. ŁOKAS

*Copernicus Astronomical Center  
Bartycka 18, 00-716 Warsaw, Poland  
E-mail: lokas@camk.edu.pl*

**ABSTRACT**

Using the two-point Edgeworth series up to second order we construct the weakly nonlinear conditional probability distribution function for the density field around an overdense region. This requires calculating the two-point analogues of the skewness parameter  $S_3$ . We test the dependence of the two-point skewness on distance from the peak for scale-free power spectra and Gaussian smoothing. The statistical features of such conditional distribution are given as the values obtained within linear theory corrected by the terms that arise due to weakly nonlinear evolution. The expected density around the peak is found to be always below the linear prediction while its rms fluctuation is always larger than in the linear case. We apply these results to the spherical model of collapse as developed by Hoffman & Shaham (1985) and find that in general the effect of weakly nonlinear interactions is to decrease the scale from which a peak gathers mass and therefore also the mass itself. In the case of open universe this results in steepening of the final profile of the virialized protoobject.

*Key words:* methods: analytical – cosmology: theory – galaxies: formation – large-scale structure of Universe

Submitted to MNRAS

# 1 Introduction

The simplest deterministic model of structure formation proposed by Gunn & Gott (1972), called the spherical model, described the evolution of an overdense region in the otherwise unperturbed, expanding Universe. It was extended by Gott (1975) and Gunn (1977) to apply to the evolution of matter around an already collapsed density perturbation superposed on a homogeneous background. The main prediction of the model (called the spherical accretion or the secondary infall model) was that the matter collapsing around the perturbation should form a halo with  $r^{-9/4}$  density profile.

It is much more realistic to assume that the progenitors of structure were not the collapsed perturbations but the local maxima (rare events) in the density field which had initially Gaussian probability distribution. This was the approach of Hoffman & Shaham (1985) (hereafter HS) who applied the secondary infall mechanism to the hierarchical clustering model. They assumed that the density peak dominates to some extent the surroundings causing the collapse of the material that is gravitationally bound to it. The initial density profile around the peak was approximated by the mean density predicted by the initial probability distribution which was assumed to be Gaussian. Thus a link was established between the statistical nature of the fluctuations and the deterministic character of the spherical model. HS considered scale-free initial power spectra of fluctuations and found that the final profiles of halos depend on the spectral index  $n$  and on the density parameter  $\Omega$ .

One of the key assumptions underlying the calculations of HS was that the matter influenced by the peak collapses onto it undisturbed by the background. This is equivalent to the statement that the peak identified with some resolution (smoothing) scale collapses while the surrounding density field is still linear i.e. its rms fluctuation at this scale is much smaller than unity. Since the rms fluctuation grows with time and decreases with the smoothing scale, this approximation might be true for very early stages of evolution or very large smoothing scales. The example of the Virgo supercluster (which has not yet collapsed) shows that this is not always the case: assuming the power spectrum  $P(k) \propto k^{-3/2}$  and knowing that at present the rms fluctuation is of the order of unity at the smoothing scale of 10 Mpc, the size of the supercluster being around 30 Mpc, one can easily estimate that the rms fluctuation at the scale of the supercluster is well in the weakly nonlinear regime.

The purpose of this paper is to present a generalization of the calculations of HS to the case of density peaks collapsing in the weakly nonlinear background. In this way we hope to account properly for the weakly nonlinear transition between the linear and strongly nonlinear phase of the evolution of the perturbation which lacked in the approach of HS. Such a generalization involves constructing the weakly nonlinear probability distribution function (PDF) of density around an overdense region. The properties of the one-point weakly nonlinear PDFs were discussed by many authors (e.g. Bernardeau & Kofman 1995; Juszkiewicz et al. 1995) and all studies confirm that the weakly nonlinear PDFs develop features which are absent in the linear phase of the evolution e.g. the skewness. Those functions describe the density field at a randomly chosen point. Here we impose the condition that the point be chosen in the vicinity of a significantly overdense region which requires constructing first the two-point weakly nonlinear PDF. Then the PDF in this point is given by the conditional probability obtained from the two point PDF with the restriction that the density in the second point (the location of the peak) is known and equal to a constant. The mean density obtained from this weakly nonlinear PDF is then taken as the initial condition for spherical collapse.

The reliability of this approach rests on the assumption that the influence of the neighbouring fluctuations can be restricted to the weakly nonlinear phase with its only outcome in the form of a changed ‘initial’ density profile that can then evolve independently of surroundings, according to the spherical model. Although it is quite obvious that the evolution of a strongly nonlinear object is governed mainly by its own gravity and is little affected by its surroundings, it is very difficult to determine precisely the moment when such a situation takes place, i.e. a moment when we should pass from the weakly nonlinear statistical description to the strongly nonlinear deterministic spherical model.

The paper is organized as follows. In Section 2 we construct the bivariate Edgeworth series and calculate the two-point skewness parameter for scale-free power-law spectra and Gaussian smoothing. In Section 3 we calculate the conditional probability distribution of the density field around a peak and discuss its properties. Section 4 provides the application of the results to the spherical collapse model. The concluding remarks follow in Section 5.

## 2 The bivariate Edgeworth series

We consider density contrast field which initially has Gaussian distribution with zero mean. The field measured at a given point will be denoted by the symbol  $\delta$  while the one measured at the distance  $r$  from the first point will be called  $\gamma$ . They can be treated as two variables, two fields in the same space. Since the fields can in general be smoothed with filters of different scales their variances can be different:  $\langle \delta^2 \rangle = \sigma^2$  and  $\langle \gamma^2 \rangle = \tau^2$ . The (auto)correlation function of these two fields is given by

$$\langle \delta(\mathbf{x}) \gamma(\mathbf{x} + \mathbf{r}) \rangle = \xi(r). \quad (1)$$

Hereafter we will consider the normalized density contrast fields  $\mu = \delta/\sigma$  and  $\nu = \gamma/\tau$ . Their variances are now equal to unity and their correlation is now given by  $\varrho = \xi/\sigma\tau$ . The quantity  $\varrho$  will be referred to as the correlation coefficient. The joint probability distribution of the two variables in the Gaussian case is

$$p(\mu, \nu) = \frac{1}{2\pi\sqrt{1-\varrho^2}} f(\mu, \nu, \varrho) \quad (2)$$

where

$$f(\mu, \nu, \varrho) = \exp \left[ -\frac{(\mu^2 - 2\varrho\mu\nu + \nu^2)}{2(1-\varrho^2)} \right]. \quad (3)$$

If the fields were uncorrelated ( $\varrho = 0$ ),  $p(\mu, \nu)$  would be just a product of two Gaussian distributions of  $\mu$  and  $\nu$ .

The purpose of this section is to generalize the joint probability distribution function in the Gaussian case (2) to the case when the density fields are weakly nonlinear and therefore departing from Gaussianity. If the rms fluctuations of the fields are small (below unity) the fields can be expanded around their linear values  $\delta_1$  and  $\gamma_1$  respectively

$$\delta = \delta_1 + \delta_2 + \delta_3 + \dots \quad (4)$$

$$\gamma = \gamma_1 + \gamma_2 + \gamma_3 + \dots \quad (5)$$

As discussed by Juszkiewicz et al. (1995) the so-called Edgeworth series provides a good approximation to the one-point PDF, except for the very tails of the distribution. Up to the

third order approximation the Edgeworth series reads

$$p(\nu) = \frac{1}{\sqrt{2\pi}} e^{-\nu^2/2} \left[ 1 + \frac{1}{3!} S_3 \sigma H_3(\nu) + \frac{1}{4!} S_4 \sigma^2 H_4(\nu) + \frac{10}{6!} S_3^2 \sigma^2 H_6(\nu) \right] \quad (6)$$

where  $S_3$  and  $S_4$  are respectively the third and fourth normalized cumulants of the density contrast field, the skewness and the kurtosis (see e.g. Bernardeau 1994; Lokas et al. 1995) and  $H_n(\nu)$  is the Hermite polynomial of the  $n$ -th order generated by

$$(-1)^n \frac{d^n}{d\nu^n} e^{-\nu^2/2} = e^{-\nu^2/2} H_n(\nu). \quad (7)$$

In the construction of the bivariate Edgeworth series we follow the work of Longuet-Higgins (1963, 1964) who considered modified Gaussian distributions of weakly nonlinear variables and applied them to statistical theory of sea waves. In the second order approximation we have

$$p(\mu, \nu) = \frac{1}{2\pi\sqrt{1-\varrho^2}} f(\mu, \nu, \varrho) \left[ 1 + \frac{1}{6} (\lambda_{30} H_{30} + 3\lambda_{21} H_{21} + 3\lambda_{12} H_{12} + \lambda_{03} H_{30}) \right] \quad (8)$$

where  $f(\mu, \nu, \varrho)$  is given by equation (3). The correlation coefficient  $\varrho$ , the Hermite polynomials  $H_{mn}$  and the two-point moments  $\lambda_{mn}$  will be discussed in the following.

## 2.1 The correlation coefficient

The autocorrelation function of density field measured at two points separated by distance  $|\mathbf{r}| = r$  can be calculated using the relation

$$\xi_R(r) = \int \frac{d^3k}{(2\pi)^3} P(k) W^2(kR) e^{i\mathbf{k}\cdot\mathbf{r}} \quad (9)$$

where  $P(k)$  is the power spectrum of the density fluctuations and the field is smoothed with a window function  $W$  of radius  $R$  which in what follows will be assumed to have a Gaussian form

$$W(kR) = e^{-k^2 R^2/2}. \quad (10)$$

In what follows we will restrict the calculations to the case when the field at both locations has the same properties and is smoothed with the same smoothing radius so that the variances are equal:  $\sigma = \tau$ .

For the scale-free power spectra

$$P(k) = Ck^n, \quad -3 \leq n \leq 1 \quad (11)$$

we obtain

$$\varrho = \frac{\xi_R(r)}{\sigma^2} = \frac{\sqrt{\pi}}{2} \frac{\Gamma(1 + \frac{n}{2})}{\Gamma(\frac{n+3}{2})} L_{n/2}^{1/2} \left( \frac{c^2}{4} \right) e^{-c^2/4} \quad (12)$$

where  $c = r/R$  and  $L_\beta^\alpha(x)$  are Laguerre polynomials. Here we have used the fact that for the scale-free power spectra (11) and Gaussian smoothing (10) the linear variance of the density PDF is given by

$$\sigma^2 = \langle \delta_1^2 \rangle = D^2(t) \int \frac{d^3k}{(2\pi)^3} P(k) W^2(kR) = CD^2(t) \frac{\Gamma(\frac{n+3}{2})}{(2\pi)^2 R^{n+3}}. \quad (13)$$

Hereafter the variance  $\langle \delta^2 \rangle$  will be always approximated by the linear value (13) which is sufficient in the construction of the two-point Edgeworth series up to second order. The result (12) takes simpler form in terms of the degenerate hypergeometric function

$$\varrho(n, c) = {}_1F_1\left(\frac{n+3}{2}, \frac{3}{2}, -\frac{c^2}{4}\right). \quad (14)$$

We see that the correlation coefficient depends on the scales  $r$  and  $R$  only via their ratio  $c$ . Upper panel of Figure 1 shows the shape of  $\varrho(c)$  for different power spectrum indices  $n = -2, -1.5, -1$ .

## 2.2 The bivariate Hermite polynomials

The quantities  $H_{mn}$  in (8) are two-dimensional analogues of the Hermite polynomials  $H_n$  appearing in the one-point Edgeworth series (6) that were generated by equation (7). The bivariate Hermite polynomials can be calculated using similar formula

$$(-1)^{m+n} \frac{d^m}{d\mu^m} \frac{d^n}{d\nu^n} f(\mu, \nu, \varrho) = f(\mu, \nu, \varrho) H_{mn}(\mu, \nu, \varrho). \quad (15)$$

The polynomials of orders needed in this calculation can be written in the form

$$H_{mn}(\mu, \nu, \varrho) = \frac{1}{(1-\varrho^2)^2} h_{mn}(\mu, \nu, \varrho) \quad (16)$$

where

$$\begin{aligned} h_{30} &= \frac{(\mu - \varrho\nu)^3}{1 - \varrho^2} - 3(\mu - \varrho\nu) \\ h_{21} &= 2\varrho(\mu - \varrho\nu) - (\nu - \varrho\mu) + \frac{(\nu - \varrho\mu)(\mu - \varrho\nu)^2}{1 - \varrho^2} \\ h_{12} &= 2\varrho(\nu - \varrho\mu) - (\mu - \varrho\nu) + \frac{(\mu - \varrho\nu)(\nu - \varrho\mu)^2}{1 - \varrho^2} \\ h_{03} &= \frac{(\nu - \varrho\mu)^3}{1 - \varrho^2} - 3(\nu - \varrho\mu). \end{aligned} \quad (17)$$

## 2.3 The two-point skewness

The coefficients  $\lambda_{ij}$  in (8) are defined by the reduced moments (cumulants)  $\kappa_{ij}$  in the following way

$$\lambda_{ij} = \frac{\kappa_{ij}}{(\kappa_{20}^i \kappa_{02}^j)^{1/2}} \quad (18)$$

while the cumulants of the fields  $\delta$  and  $\gamma$  are given by the connected part of the moments

$$\kappa_{ij} = \langle \delta^i \gamma^j \rangle_c. \quad (19)$$

Using the perturbative expansion of the fields, equations (4)-(5), we find up to second order

$$\begin{aligned} \kappa_{30} &= \langle \delta_1^3 \rangle + 3\langle \delta_1^2 \delta_2 \rangle \\ \kappa_{21} &= \langle \delta_1^2 \gamma_2 \rangle + 2\langle \delta_1 \delta_2 \gamma_1 \rangle \\ \kappa_{12} &= \langle \delta_2 \gamma_1^2 \rangle + 2\langle \delta_1 \gamma_1 \gamma_2 \rangle \\ \kappa_{03} &= \langle \gamma_1^3 \rangle + 3\langle \gamma_1^2 \gamma_2 \rangle. \end{aligned} \quad (20)$$

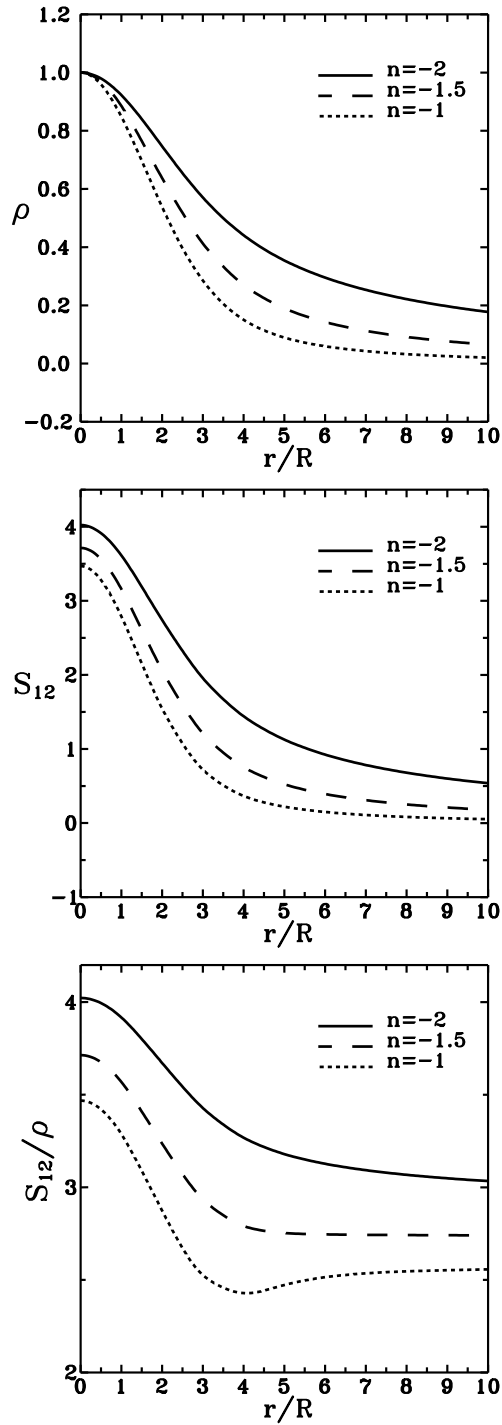


Figure 1: The values of the correlation coefficient  $\rho$ , the two-point skewness  $S_{12}$  and the ratio  $S_{12}/\rho$  as functions of the distance between the two points (in units of the smoothing scale),  $c = r/R$ , for different power spectra.

The moments  $\kappa_{20}$  and  $\kappa_{02}$  are just the variances  $\langle \delta^2 \rangle$  and  $\langle \gamma^2 \rangle$  respectively, which, as stated before, can be both approximated by the linear value  $\sigma^2$  given by equation (13).

The moments  $\kappa_{30}$  and  $\kappa_{03}$  are related to the ordinary one-point skewness parameters (see e.g. Peebles 1980; Juszkiewicz et al. 1993). For Gaussian fields  $\langle \delta_1^3 \rangle = 0$ , and we have

$$\kappa_{30} = 3\langle \delta_1^2 \delta_2 \rangle = S_3 \sigma^4 \quad (21)$$

where  $S_3$  is the dimensionless skewness parameter which for a Gaussian filter depends on the spectral index  $n$  in the following way (Łokas et al. 1995)

$$S_3 = 3 {}_2F_1\left(\frac{n+3}{2}, \frac{n+3}{2}, \frac{3}{2}, \frac{1}{4}\right) - \left(n + \frac{8}{7}\right) {}_2F_1\left(\frac{n+3}{2}, \frac{n+3}{2}, \frac{5}{2}, \frac{1}{4}\right). \quad (22)$$

The other one-point moment  $\kappa_{03} = S_3 \tau^4$  but since we have already put  $\tau = \sigma$  we have  $\kappa_{03} = \kappa_{30}$ .

The two-point moments  $\kappa_{21}$  and  $\kappa_{12}$  can be calculated using the same method as in the case of one-point skewness (Łokas et al. 1995) but now we have to keep the dependence of the moments on distance  $r = |\mathbf{r}|$ . The two-point moments also scale as  $\sigma^4$  so it is convenient to calculate them in the normalized form. Using equation (13) we have for  $\kappa_{21}/\sigma^4$

$$\begin{aligned} \frac{\langle \delta_1^2 \gamma_2 \rangle(r)}{\sigma^4} &= \frac{1}{448\pi^6 R^{2(n+3)} \sigma^4} \int d^3 p \int d^3 q W(p) W(q) W(|\mathbf{p} + \mathbf{q}|) e^{i(\mathbf{p} + \mathbf{q}) \cdot \mathbf{r}} \times \\ &\times P(p) P(q) J(\mathbf{p} + \mathbf{q}, \mathbf{p}, \mathbf{q}) \end{aligned} \quad (23)$$

and

$$\begin{aligned} \frac{2\langle \delta_1 \delta_2 \gamma_1 \rangle(r)}{\sigma^4} &= \frac{1}{224\pi^6 R^{2(n+3)} \sigma^4} \int d^3 p \int d^3 q W(p) W(q) W(|\mathbf{p} + \mathbf{q}|) e^{i\mathbf{p} \cdot \mathbf{r}} \times \\ &\times P(p) P(q) J(\mathbf{p} + \mathbf{q}, \mathbf{p}, \mathbf{q}) \end{aligned} \quad (24)$$

where  $J$  is the kernel of the second order perturbative solution for density field. The integrals (23) and (24) will be evaluated for scale-free power spectra (11) and Gaussian smoothing (10). The simplest way to perform the integrals in (23) is to change variables from  $\mathbf{p}, \mathbf{q}$  to  $\mathbf{l}, \mathbf{p}$  so that  $\mathbf{p} + \mathbf{q} = \mathbf{l}$  and  $\mathbf{l} \cdot \mathbf{p} = l p \beta$ . Together with the expression for the variance (13) this produces

$$\begin{aligned} \frac{\langle \delta_1^2 \gamma_2 \rangle(c)}{\sigma^4} &= \frac{2}{7 \Gamma^2(\frac{n+3}{2}) c} \int dp \int dl \sin(cl) p^{n+2} l e^{-l^2 - p^2} \times \\ &\times \int_{-1}^1 d\beta J(l, p, \beta) (l^2 + p^2 - 2lp\beta)^{n/2} e^{lp\beta} \end{aligned} \quad (25)$$

where  $c = r/R$  as before. The integration over the angular variable  $\beta$  can still be done analytically for integer or half-integer values of the spectral index  $n$ . The remaining integrations are done numerically. In the case of (24) the integration over angular variables gives

$$\begin{aligned} \frac{2\langle \delta_1 \delta_2 \gamma_1 \rangle(c)}{\sigma^4} &= \frac{8\sqrt{\pi}}{\sqrt{2} \Gamma^2(\frac{n+3}{2}) c} \int dp \int dq \sin(cp) p^{n+1/2} q^{n+3/2} e^{-p^2 - q^2} \times \\ &\times \left[ \frac{34}{21} I_{1/2}(pq) - \left(\frac{p}{q} + \frac{q}{p}\right) I_{3/2}(pq) + \frac{8}{21} I_{5/2}(pq) \right]. \end{aligned} \quad (26)$$

By using the expansion of Bessel functions

$$I_\nu(z) = \sum_{m=0}^{\infty} \frac{1}{m! \Gamma(\nu + m + 1)} \left(\frac{z}{2}\right)^{\nu+2m} \quad (27)$$

and the facts that

$$\int_0^\infty q^a e^{-q^2} dq = \frac{1}{2} \Gamma\left(\frac{a+1}{2}\right) \quad \text{for } a > -1 \quad (28)$$

$$\int_0^\infty p^b e^{-p^2} \sin(cp) dp = \frac{c}{2} \Gamma\left(1 + \frac{b}{2}\right) {}_1F_1\left(1 + \frac{b}{2}; \frac{3}{2}; -\frac{c^2}{4}\right) \quad \text{for } b > -2 \quad (29)$$

we obtain the result in the form of a series of combination of gamma and degenerate hypergeometric functions or Laguerre polynomials

$$\begin{aligned} \frac{2\langle\delta_1\delta_2\gamma_1\rangle(c)}{\sigma^4} &= \frac{\pi}{2\Gamma^2(\frac{n+3}{2})} e^{-c^2/4} \sum_{m=0}^\infty \frac{\Gamma(\frac{n+3}{2} + m)}{m! 2^{2m}} \times \\ &\times \left\{ \frac{34}{21} \frac{\Gamma(\frac{n+2}{2} + m)}{\Gamma(m + \frac{3}{2})} L_{n/2+m}^{1/2}\left(\frac{c^2}{4}\right) \right. \\ &- \frac{1}{2\Gamma(m + \frac{5}{2})} \left[ \Gamma\left(\frac{n+4}{2} + m\right) L_{n/2+m+1}^{1/2}\left(\frac{c^2}{4}\right) \right. \\ &+ \left. \left. \left(\frac{n+3}{2} + m\right) \Gamma\left(\frac{n+2}{2} + m\right) L_{n/2+m}^{1/2}\left(\frac{c^2}{4}\right) \right] \right. \\ &+ \left. \left. \frac{8}{21} \frac{(\frac{n+3}{2} + m)\Gamma(\frac{n+4}{2} + m)}{4\Gamma(m + \frac{7}{2})} L_{n/2+m+1}^{1/2}\left(\frac{c^2}{4}\right) \right\}. \end{aligned} \quad (30)$$

The values of

$$S_{21} = \frac{\kappa_{21}}{\sigma^4} \quad (31)$$

will be hereafter called the two-point skewness parameter. Because of the symmetry between the two locations we obviously have  $S_{12} = S_{21}$ . In the following calculations we will therefore use only the symbol  $S_{12}$ . The numerical values of  $S_{12}$  for different values of  $c$  and  $n = -2, -1.5, -1$  are given in Table 1 and plotted in the middle panel of Figure 1.

The lower panel of Figure 1 shows the ratio  $S_{12}/\varrho$ . As discussed by Bernardeau (1996) for the case of top-hat filter such quantity should approach a constant at  $c \rightarrow \infty$ . Figure 1 shows that the same behaviour is observed for Gaussian filtering. Using diagrammatic representations of the two-point moments Bernardeau (1996) has shown that the part of  $S_{12}$  given by equation (23) behaves like  $\varrho^2$  in this limit and therefore is negligible compared to the part given by equation (24) which behaves like  $\varrho$ . For large  $c$  the value of the sum in (30) is perfectly approximated by the  $m = 0$  element of the series and we find

$$S_{12} = s_{12}\varrho \quad (32)$$

where

$$s_{12} = \frac{47}{21} - \frac{n}{3}. \quad (33)$$

It is worth noting that the moment  $s_{12}$  given by equation (33) is exactly equal to the corresponding quantity  $C_{2,1}$  calculated by Bernardeau (1996) for scale-free power spectra and top-hat smoothing.

For  $n = -2, -1.5, -1$  the numerical values of  $s_{12}(n)$  are respectively: 2.90, 2.74 and 2.57. It is seen in Figure 1 that the values of  $S_{12}/\varrho$  indeed approach them for large  $c$ . The value of  $S_{12}$  is well approximated by the one given by equation (32) within 10% for  $c > 4$  (and the approximation works much better for  $n = -1$  and  $n = -1.5$  than for  $n = -2$ ). In the following, however, we will

$c = r/R$	$S_{12}$		
	$n = -2$	$n = -1.5$	$n = -1$
0	4.022	3.714	3.468
0.01	4.022	3.714	3.468
0.1	4.018	3.708	3.460
0.5	3.913	3.563	3.282
1	3.614	3.159	2.790
2	2.742	2.062	1.547
3	1.957	1.212	0.7212
4	1.441	0.7545	0.3659
5	1.126	0.5226	0.2206
6	0.9237	0.3914	0.1494
7	0.7830	0.3081	0.1084
8	0.6796	0.2510	0.08233
9	0.6003	0.2097	0.06471
10	0.5377	0.1787	0.05222

Table 1: The values of the two-point skewness parameter  $S_{12}$  for density field as a function of the spectral index  $n$  and  $c = r/R$ .

be also interested in the region of  $c$  of the order of few, where this approximation is not sufficient and cannot be adopted.

In the limit of  $c \rightarrow 0$ , which is equivalent to  $r \rightarrow 0$ , the two points at which we measure the density field converge and we expect that the two-point skewness reproduces the one-point value of  $S_3$  given by equation (22). As Table 1 and Figure 1 prove this is indeed the case. In this limit the two parts (23) and (24) have comparable contributions:  $S_3/3$  and  $2S_3/3$  respectively.

Using the results of this section the bivariate Edgeworth series (8) can be rewritten in the following way

$$\begin{aligned}
p(\mu, \nu) &= \frac{1}{2\pi\sqrt{1-\varrho^2}} f(\mu, \nu, \varrho) \\
&\times \left\{ 1 + \frac{\sigma}{6(1-\varrho^2)^2} [S_3(h_{30} + h_{03}) + 3S_{12}(h_{12} + h_{21})] \right\}.
\end{aligned}
\tag{34}$$

### 3 Conditional probability distribution around a peak

Let us now suppose that the value of one variable is known:  $\nu = a$ . The conditional probability distribution of the other variable is defined as

$$p(\mu, \nu = a) = \frac{p(\mu, a)}{\int_{-\infty}^{+\infty} p(\mu, a) d\mu}
\tag{35}$$

where the nominator is the bivariate distribution with the second variable put equal to a constant and the denominator is the marginal distribution of the variable  $\nu = a$ .

In the case of two-point Gaussian distribution (2) the resulting conditional distribution for  $\mu$

reads

$$p(\mu, \nu = a) = \frac{1}{\sqrt{2\pi(1-\varrho^2)}} \exp \left[ -\frac{(\mu - \varrho a)^2}{2(1-\varrho^2)} \right]. \quad (36)$$

This is again a Gaussian but the variance was changed from unity to  $1 - \varrho^2$  and the mean value of  $\mu$  was moved from zero to  $\mu = \varrho a$ .

In the case of two-point Edgeworth series (34) the conditional distribution of  $\mu$ , provided the value of  $\nu$  is known and equal to  $a$ , is obtained from equation (35) using the marginal distribution of  $\nu$

$$\int_{-\infty}^{+\infty} p(\mu, \nu = a) d\mu = \frac{1}{\sqrt{2\pi}} e^{-a^2/2} \left[ 1 + \frac{S_3\sigma}{6}(a^3 - 3a) \right] \quad (37)$$

which is just the one-point Edgeworth series (6) up to second order with  $\nu = a$ . Since only the lowest order correction in the Edgeworth series was introduced the result must be expanded in powers of  $\sigma$  and only the term linear in  $\sigma$  should be kept

$$p(\mu, \nu = a) = \frac{1}{\sqrt{2\pi(1-\varrho^2)}} \exp \left[ -\frac{(\mu - \varrho a)^2}{2(1-\varrho^2)} \right] \times \quad (38)$$

$$\times \left\{ 1 + \frac{\sigma}{6(1-\varrho^2)^2} [S_3(h_{30} + h_{03}) + 3S_{12}(h_{12} + h_{21})] - \frac{S_3\sigma}{6}(a^3 - 3a) \right\}$$

where  $h_{mn} = h_{mn}(\mu, a, \varrho)$  are given by equations (17).

First let us check the behaviour of the conditional probability (38) in the limit of the correlation coefficient  $\varrho \rightarrow 0$  i.e. when the two considered points are separated by large distance and therefore uncorrelated. According to the results of the previous section in this limit also  $S_{12} \rightarrow 0$  and the distribution (38) becomes

$$p(\mu, \nu = a)|_{\varrho \rightarrow 0} = \frac{1}{\sqrt{2\pi}} e^{-\mu^2/2} \left[ 1 + \frac{S_3\sigma}{6}(\mu^3 - 3\mu) \right] \quad (39)$$

which is just the one-point Edgeworth series (6), as expected. The probability distribution for the density field is not supposed to depend on a particular value of density contrast at infinite distance.

In order to test the behaviour of the distribution (38) for different parameters  $\varrho$ ,  $a$  and  $\sigma$  we calculate its lowest order moments with respect to the mean value  $\langle \mu \rangle_E$  (the subscript  $E$  will identify the quantities obtained for the distribution (38)) and compare them with the corresponding quantities of the Gaussian conditional distribution (36). Let us recall that for Gaussian distribution we found (in agreement with Dekel 1981, Peebles 1984 and HS)

$$\langle \mu \rangle_G = \varrho a \quad (40)$$

$$\langle (\mu - \langle \mu \rangle)^2 \rangle_G = 1 - \varrho^2 \quad (41)$$

$$\langle (\mu - \langle \mu \rangle)^3 \rangle_G = 0. \quad (42)$$

After tedious but straightforward calculations for the Edgeworth conditional probability (38) we get

$$\langle \mu \rangle_E = \varrho a + \frac{\sigma}{2}(a^2 - 1)(S_{12} - \varrho S_3) \quad (43)$$

$$\langle (\mu - \langle \mu \rangle)^2 \rangle_E = 1 - \varrho^2 + \sigma a (S_{12} - 2\varrho S_{12} + \varrho^2 S_3) \quad (44)$$

$$\langle (\mu - \langle \mu \rangle)^3 \rangle_E = \sigma (S_3 - 3\varrho S_{12} + 3\varrho^2 S_{12} - \varrho^3 S_3). \quad (45)$$

From equation (44) we also have the dispersion to the lowest order in  $\sigma$

$$\langle(\mu - \langle\mu\rangle)^2\rangle_E^{1/2} = \sqrt{1 - \varrho^2} + \frac{\sigma a (S_{12} - 2\varrho S_{12} + \varrho^2 S_3)}{2\sqrt{1 - \varrho^2}}. \quad (46)$$

Clearly the characteristics of the conditional Edgeworth distribution are given by the Gaussian ones plus correction terms proportional to  $\sigma$  and a function of  $a$  (except for the third moment which is independent of  $a$ ). As shown earlier in equation (39) in the limit of  $\varrho \rightarrow 0$  the conditional Edgeworth distribution approaches one-point Edgeworth series. This must also apply to its moments. Using the fact that at small  $\varrho$  the values of two-point skewness  $S_{12}$  vanish we again find that in this limit the third order moment (45) approaches the value of the one-point Edgeworth series,  $S_3\sigma$ . The same is true for the lower moments (43) and (44).

An independent check of the results (43)-(45) is provided in the limit of  $\varrho \rightarrow 1$ . Then the distribution  $p(\mu, \nu = a)$  should approach the Dirac's delta function,  $\delta_D(\mu - a)$ , with the mean equal to  $a$  and the second and third moment equal to zero. Recalling that in this limit  $S_{12} \rightarrow S_3$  such results can be immediately reproduced from equations (43)-(45).

An interesting application of these results from the point of view of the theory of structure formation is to study the density distribution around an overdense region. Although the results presented so far apply to arbitrary values of  $a$  we will from now on focus on regions which are able to dominate their surroundings, that is their density contrast is bigger than one standard deviation. This corresponds to assuming  $a > 1$ . A region of such overdensity will be called a peak although it might not be a maximum in a strict mathematical sense. However, we expect that points of  $a \gg 1$  most probably correspond to local maxima. As reasoned by HS, this is also true for mild values of  $a \gtrsim 1$  (see also Adler 1981).

If  $a > 1$  the moments (40)-(45) can be interpreted as characteristics of the density distribution around a density peak. The Gaussian values are the well known results of linear theory while the values for the Edgeworth conditional distribution provide the corrections introduced by the fact that the field on a given smoothing scale has become weakly nonlinear. The direction of the effect depends on the numerical values of the one-point and two-point skewness parameters and the correlation coefficient.

It is clear from Figure 1 that for the spectral indices considered here ( $n = -2, -1.5, -1$ ) and nonzero distance from the peak we have  $S_{12}/\varrho < S_3$  which can be rewritten as

$$S_{12} - \varrho S_3 < 0. \quad (47)$$

This proves that according to equation (43) for  $a > 1$  the correction to the mean normalized density with respect to the Gaussian value is always negative. Figure 2 shows the expected normalized density contrast  $\langle\mu\rangle$  for the Edgeworth (43) and Gaussian (40) conditional distributions as a function of the distance from the peak (in units of the smoothing scale),  $c = r/R$ . Each panel shows results for different scale-free power spectrum with spectral index  $n = -2, -1.5, -1$ . In each panel the Edgeworth results are plotted as thicker solid lines while the thinner dashed lines show the Gaussian ones. The four pairs of lines in each panel correspond from bottom to top to the four chosen values of the peak's height:  $a = 1, 2, 3, 4$  (for  $a = 1$  the results are the same in both Gaussian and Edgeworth cases). The Edgeworth results are always below the Gaussian values so it is clear that the effect of weakly nonlinear interactions is to decrease the expected density around an overdense region. Equation (43) shows explicitly that the effect grows with  $a$  and  $\sigma$ .

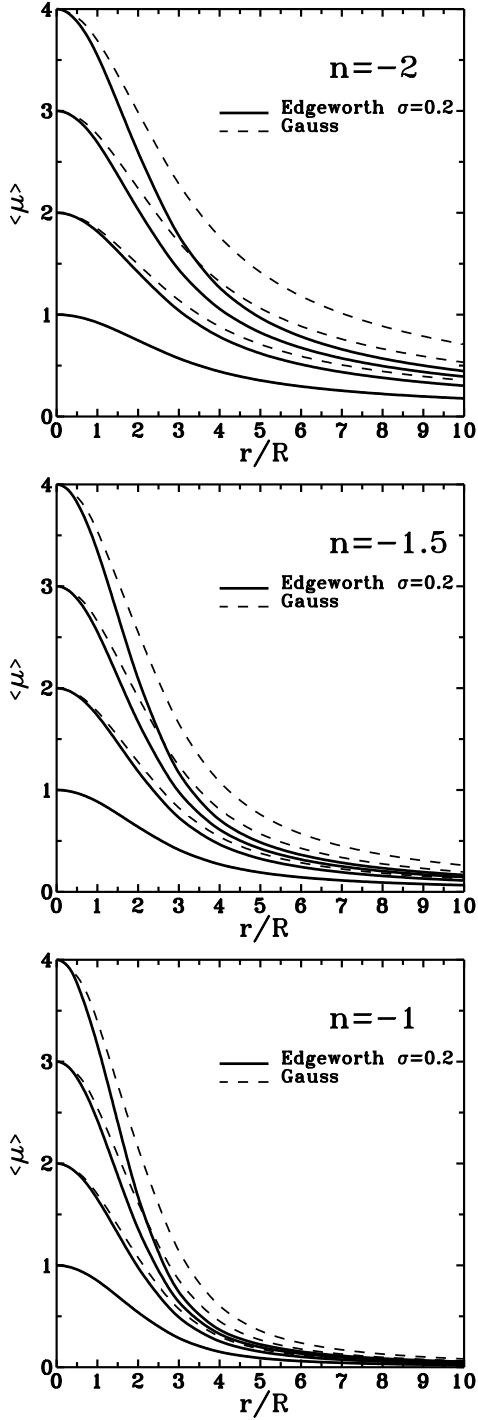


Figure 2: The mean normalized density contrast as a function of  $c = r/R$ . The dashed lines correspond to the Gaussian case while the solid ones show the results obtained from the Edgeworth approximation with  $\sigma = 0.2$ . Each panel shows results for  $a = 1, 2, 3, 4$  and different power spectrum.

Juszkiewicz et al. (1995) have tested the third order Edgeworth approximation against N-body simulations and found that it is accurate for density contrast up to  $\delta = a\sigma = 1$ . Here we are using only the second order approximation so the range of validity of these results is probably even more restricted. Therefore in the following it will be assumed that  $a\sigma$  is always below unity. All the Edgeworth results in Figure 2 are given for  $\sigma = 0.2$ . At this value of the rms density fluctuation we still have  $a\sigma < 1$  even for  $a = 4$  so we can expect the Edgeworth series to be a good approximation.

In the case of the variance the weakly nonlinear corrections work in the opposite direction: their effect is to increase the value of the variance (or dispersion) with respect to the linear case, because for the power spectra considered here (and nonzero distances from the peak) we always have

$$S_{12} - 2\varrho S_{12} + \varrho^2 S_3 = (1 - \varrho)S_{12} + \varrho(\varrho S_3 - S_{12}) > 0 \quad (48)$$

where the inequality (47) was used. The effect grows linearly with  $\sigma$  and  $a$  as equation (44) states. In Figure 3 we plot the dispersion of the conditional Edgeworth distribution (46) and the Gaussian dispersion which is independent of  $a$  and equal to  $\sqrt{1 - \varrho^2}$ . The quantities are shown as functions of  $c = r/R$  for  $\sigma = 0.2$ ,  $a = 1, 2, 3, 4$  and different power spectra. As in Figure 2 the thicker solid lines in each panel correspond to the Edgeworth results and the thinner dashed lines to the Gaussian ones. Although the Gaussian dispersion is always below unity and approaches it at large  $c$ , the Edgeworth values reach a maximum, which is above unity at  $c$  of the order of a few and then decrease down to unity at large distances.

An important conclusion coming from the behaviour of weakly nonlinear expected density and its variance is the following. It is clear that a local density peak that rises significantly above the noise should gravitationally dominate its surroundings out to some distance. A reasonable measure of the distance, up to which a coherent structure around the peak is expected, is the scale  $r_{coh}$  at which

$$\langle \mu \rangle = \langle (\mu - \langle \mu \rangle)^2 \rangle^{1/2}. \quad (49)$$

Because of smoothing it is more convenient to measure the distance  $r$  in units of the smoothing scale  $R$  so in what follows we will use  $c_{coh} = r_{coh}/R$  instead of  $r_{coh}$ . The mean  $\langle \mu \rangle$  as a function of  $c$  up to  $c_{coh}$  may be therefore treated as the density profile of matter that is bound to the peak in a statistical sense.

In the Gaussian case equation (49) leads to  $\varrho(n, c_{coh}) = 1/\sqrt{a^2 + 1}$  which can be solved numerically for  $c_{coh}$  given the shape of  $\varrho$ , equation (14). Finding  $c_{coh}$  in the case of Edgeworth approximation requires fitting the function  $S_{12}(c)$  and then equation (49) can also be solved numerically. The results for both cases are shown in Figure 4 as dependent on the height of the peak  $a$ , for three different values of  $\sigma = 0.05, 0.1, 0.2$  and three spectral indices  $n = -2, -1.5, -1$ . Since the mean density is decreased and the dispersion is increased the effect of nonlinearity is always to decrease the coherence length. The magnitude of the effect grows with the rms fluctuation  $\sigma$ . Therefore the density field around a peak embedded in the weakly nonlinear field decorrelates much faster with distance than in the linear case.

Note that the scale of each panel in Figure 4 is different: the values of  $c_{coh}$  are generally significantly larger for lower spectral indices but this reflects mainly the amount of large-scale power in the initial linear power spectrum. To take this into account the weakly nonlinear coherence length should be compared to the corresponding Gaussian one. Then the dependence on the power spectrum is clear: for a given  $a$  and  $\sigma$  the change in the value of  $c_{coh}$  with respect to the Gaussian one is larger for lower spectral indices. For example for  $a = 3$  and  $\sigma = 0.1$  the

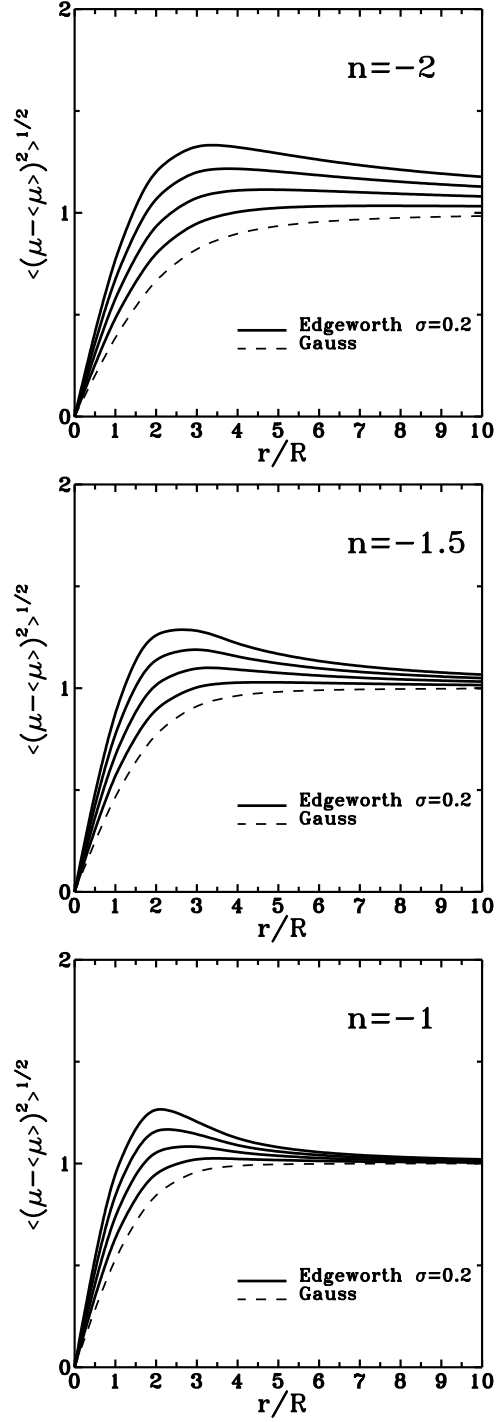


Figure 3: The dispersion of the normalized density contrast as a function of the distance from the peak,  $c = r/R$ . The dashed line in each panel shows Gaussian results which are independent of the peak's height while the four solid lines correspond to the results obtained from the Edgeworth approximation with  $\sigma = 0.2$  and  $a = 1, 2, 3, 4$ . Each panel shows results for different power spectrum.

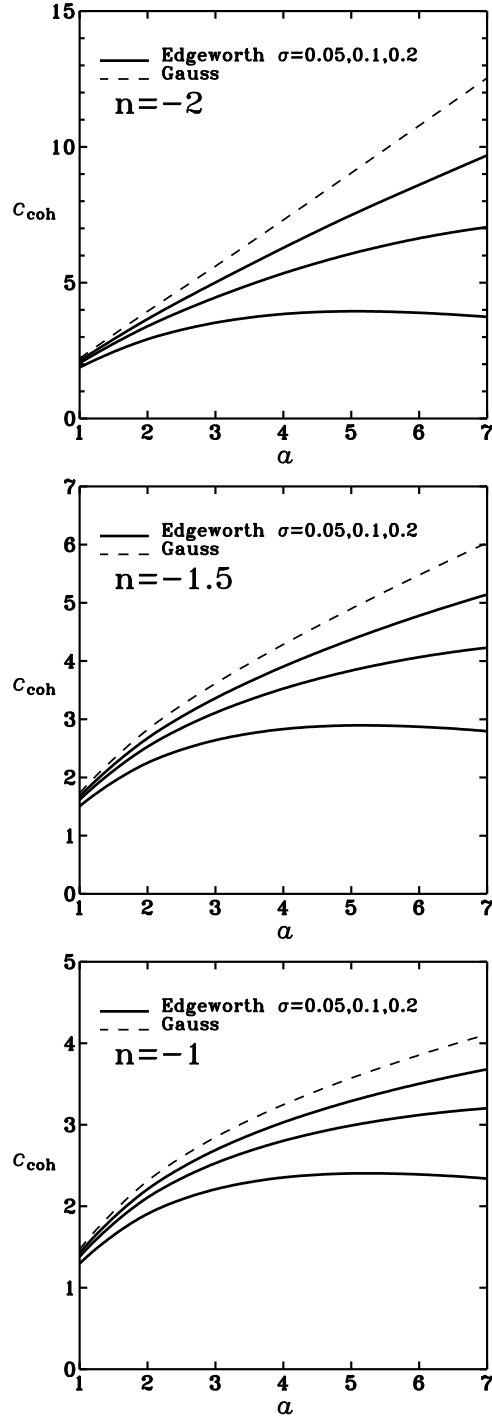


Figure 4: The length of coherence (in units of the smoothing scale) defined by equation (49) as a function of the peak's height,  $a$ . The dashed line in each panel shows the results in the Gaussian case. The solid lines correspond to the results obtained from the Edgeworth approximation with  $\sigma = 0.05, 0.1, 0.2$ , with larger  $\sigma$  producing a curve that departs more from the Gaussian one.

weakly nonlinear  $c_{coh}$  is decreased with respect to the linear value by 11%, 14% and 21% for  $n = -1, -1.5, -2$  respectively.

In general the coherence length grows with the height of the peak,  $a$ , which is reasonable: higher peaks should dominate their surroundings to farther extent. However, for largest values of  $\sigma = 0.2$  we observe that the curves in Figure 4 have a maximum at  $a \approx 5$ . Since in this case  $a\sigma = 1$  it is probably the effect of breakdown of the Edgeworth approximation.

Another important quantity to characterize the conditional distribution (38) is the third moment (45). For the Gaussian distribution this moment is always equal to zero, while for the weakly nonlinear case a good measure of it (and the asymmetry of the distribution) is the quantity

$$\frac{\langle(\mu - \langle\mu\rangle)^3\rangle_E}{\langle(\mu - \langle\mu\rangle)^2\rangle_E^{3/2}} = \frac{\sigma (S_3 - 3\varrho S_{12} + 3\varrho^2 S_{12} - \varrho^3 S_3)}{(1 - \varrho^2)^{3/2}} \quad (50)$$

where we have used equations (44)-(45), the quantity was expanded in powers of  $\sigma$  and only the term linear in  $\sigma$  was kept.

Figure 5 shows the values of the normalized third moment (50) as a function of  $c$  for  $\sigma = 0.1$  and different power spectra. It is obvious that the shape of the curves would be the same for any other  $\sigma$ . It is worth noting that the value (50) which provides the lowest order correction to the Gaussian case does not depend on the height of the peak,  $a$ . The third moment normalized in such way grows with  $c$  for all considered spectral indices. For large  $c$  the values (at a given  $\sigma$  and  $c$ ) are higher for lower spectral indices and they approach those of the one-point Edgeworth series,  $S_3\sigma$ , with  $S_3$  given by equation (22): 4.022, 3.714 and 3.468 respectively for  $n = -2, -1.5$  and  $-1$ . It is interesting that up to  $c \approx 3$  the dependence on the spectral index is weak but opposite: the third moment grows with  $n$ .

## 4 Application to spherical collapse

The dynamical evolution of matter at the distance  $c_i$  from the peak is determined by the mean cumulative density perturbation within  $c_i$  which is given by

$$\Delta_i(c_i) = \frac{3}{c_i^3} \int_0^{c_i} \delta(c) c^2 dc \quad (51)$$

where we put  $\delta(c) = \sigma\langle\mu\rangle$  with  $\langle\mu\rangle$  given by equations (40) and (43) in Gaussian and Edgeworth case respectively. In the linear case the function  $\Delta_i(c_i)$  is well approximated by

$$\Delta_{i,G}(c_i) = \begin{cases} a\sigma & \text{for } c_i \ll 1 \\ a\sigma h(n) c_i^{-(n+3)} & \text{for } c_i \gg 1 \end{cases} \quad (52)$$

where  $h(n)$  is a numerical factor. Its values for different spectral indices are given in Table 2. The approximation at large  $c_i$  is accurate to within 10% for  $c_i \geq 5$ .

In the weakly nonlinear case equations (43) and (32) give

$$\Delta_{i,E}(c_i) = \begin{cases} a\sigma & \text{for } c_i \ll 1 \\ a\sigma h(n) [1 - \sigma(S_3 - s_{12})(a^2 - 1)/(2a)] c_i^{-(n+3)} & \text{for } c_i \gg 1 \end{cases} \quad (53)$$

where  $S_3$  and  $s_{12}$  are given by equations (22) and (33) respectively. The factor  $S_3 - s_{12}$  is of the order of unity; the exact numerical values for different  $n$  are given in Table 2. Equation (53)

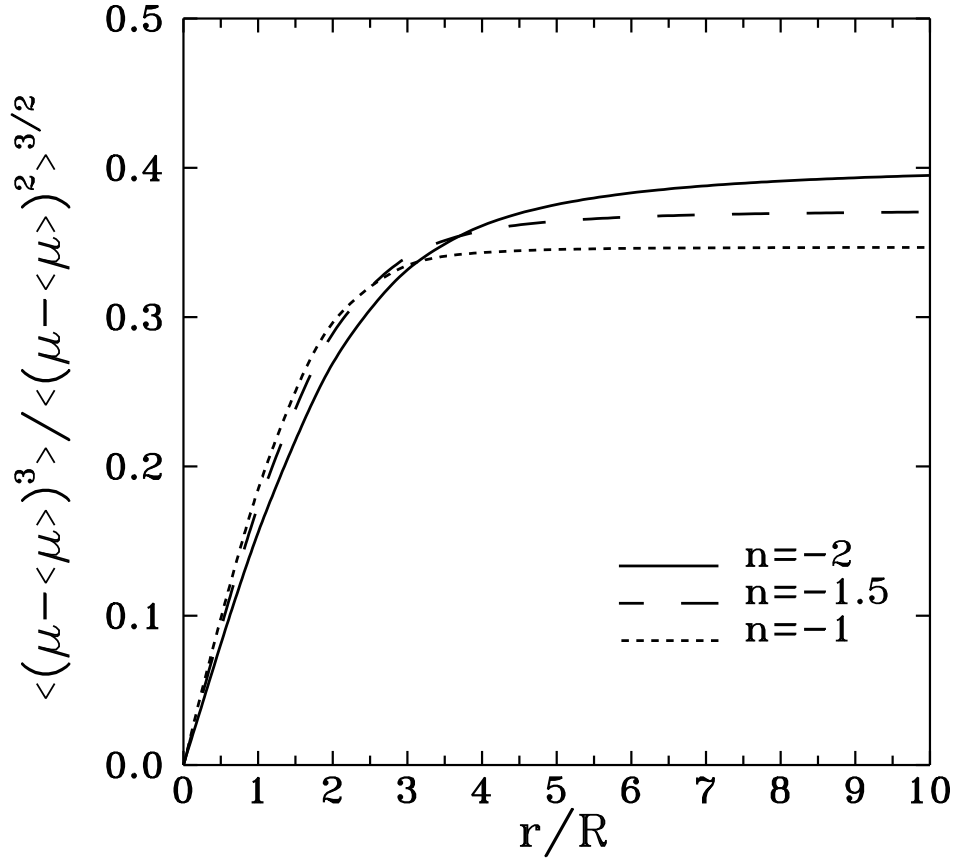


Figure 5: The properly normalized third moment of the conditional distribution as a function of the distance from the peak,  $c = r/R$ , for  $\sigma = 0.1$ . Different lines show results for different power spectra. At large distances the curves flatten to reach the limiting values of  $S_3\sigma$ .

$n$	$h$	$S_3 - s_{12}$
-3.0	1.	1.619
-2.5	1.659	1.329
-2.0	2.659	1.117
-1.5	4.091	0.9757
-1.0	6.	0.8966
-0.5	8.296	0.8747
0.0	10.63	0.9064
0.5	12.27	0.9897
1.0	12.	1.124

Table 2: The values of the parameters  $h$  and  $S_3 - s_{12}$  as functions of the spectral index  $n$ .

shows that in the limit of large  $c_i$  weakly nonlinear interactions do not change the slope of the average initial density profile. Instead the effective height of the peak is changed: the profile (53) at large  $c_i$  can be viewed as a linear profile (52) with the effective height of the peak

$$a_{eff} = a \left[ 1 - \frac{\sigma(S_3 - s_{12})(a^2 - 1)}{2a} \right]. \quad (54)$$

If we now assume that the matter of average density  $\Delta_i$  within distance  $c_i$  from the peak collapses undisturbed onto the peak, the spherical model can be applied. In what follows we compare the predictions of the spherical model with Gaussian initial conditions to the ones obtained with the initial conditions settled by the Edgeworth approximation.

According to the spherical model the radius of maximum expansion is related to the initial radius of the shell  $r_i$  in the following way

$$r_m = r_i \frac{\Delta_i + 1}{\Delta_i - \delta_c} \quad (55)$$

where  $\delta_c = \Omega_i^{-1} - 1$  and  $\Omega_i$  is the density parameter at some initial epoch. The maximal radius is related to the radius of the shell after virialization,  $r$ , in the following way

$$r = f r_m, \quad (56)$$

where  $f$  is of the order of 1/2.

From now on we will focus on the analytically tractable case of large  $c_i$  where the corresponding  $\Delta_i$  are much less than unity. Combining (55) and (56), expressing distances in units of the smoothing scale  $R$ ,  $r = cR$ , and expanding in powers of  $\Delta_i$  we have

$$\frac{c_i}{c} = \frac{1}{f} \frac{\Delta_i - \delta_c}{\Delta_i + 1} = \frac{1}{f} [-\delta_c + (1 + \delta_c)\Delta_i + \mathcal{O}(\Delta_i^2)]. \quad (57)$$

The expansion (57) is in fact an expansion in powers of  $c_i^{-(n+3)}$  as a small parameter but it is equivalent to the expansion in  $\sigma$  if the terms of the order of  $c_i^{-2(n+3)}$  and higher are neglected.

The value of  $\delta_c$  defines the radius  $c_0$  of the shell, the total energy of which vanishes. All shells of radii  $c_i < c_0$  are gravitationally bound to the peak and will eventually collapse onto it. The

condition of vanishing energy leads to  $\Delta_i(c_0) = \delta_c$  and in the linear case we have

$$c_{0,G} = \left[ \frac{a\sigma h(n)}{\delta_c} \right]^{1/(n+3)} \quad (58)$$

while in the weakly nonlinear approximation

$$c_{0,E} = \left[ \frac{a_{eff}\sigma h(n)}{\delta_c} \right]^{1/(n+3)} = c_{0,G} \left[ 1 - \frac{\sigma(S_3 - s_{12})(a^2 - 1)}{2a(n+3)} \right]. \quad (59)$$

The weakly nonlinear  $c_0$  is therefore decreased with respect to the linear one.

Since all shells which are gravitationally bound to the peak have  $\Delta_i(c_i) > \delta_c$  the term  $\delta_c \Delta_i$  in equation (57) can be neglected as being of the order of  $\Delta_i^2$  and we have

$$\frac{c_i}{c} = \frac{\delta_c}{f} \left[ \left( \frac{c_0}{c_i} \right)^{n+3} - 1 \right]. \quad (60)$$

The density run of the collapsed object can be estimated by assuming that the material originally at the shell of radius  $c_i$  ends up at  $c$  so that

$$\rho(c)c^2 dc = \rho_i(c_i)c_i^2 dc_i. \quad (61)$$

The initial density of the shell of radius  $c_i$

$$\rho_i(c_i) = \rho_{b,i}[1 + \delta_i(c_i)], \quad (62)$$

can be approximated by  $\rho_{b,i}$ , the background density at the initial epoch, since at large  $c_i$  considered here the expected value of  $\delta_i$  is very small in linear case and in fact even smaller in the weakly nonlinear approximation as was demonstrated in equation (43). The density profile is therefore in general given by

$$\rho(c) = \rho_{b,i} \left( \frac{\delta_c}{f} \right)^3 \frac{[(c_0/c_i)^{n+3} - 1]^4}{(n+4)(c_0/c_i)^{n+3} - 1}. \quad (63)$$

In the two limiting cases of interest that is of  $c_i$  much smaller than and comparable to  $c_0$  we have

$$\rho(c) = \frac{\rho_{b,i}}{n+4} \left( \frac{\delta_c}{f} \right)^{3/(n+4)} \left( \frac{c_0}{c} \right)^{3(n+3)/(n+4)} \quad \text{for } c_i \ll c_0 \quad (64)$$

$$\rho(c) = \frac{\rho_{b,i}}{n+3} \frac{f}{\delta_c} \left( \frac{c_0}{c} \right)^4 \quad \text{for } c_i \leq c_0. \quad (65)$$

The dependence of  $\rho(c)$  on the ratio  $c_0/c$  and the form of the two limiting cases are then the same in the weakly nonlinear as in the linear case discussed by HS. When  $c_0$  is very large or very small the weakly nonlinear corrections will not affect much the linear results and the slopes (64) and (65) will be preserved. The case of  $c_0 \rightarrow \infty$  corresponds to  $\Omega_i = 1$ . If at present we have  $\Omega_0 = 1$  then surely in the past also  $\Omega_i = 1$  and all profiles should have the asymptotic form (64). If the present universe is open the profile depends on the collapse time of the structure: the structures that collapsed later (with lower  $\Omega_i$ ) should have smaller  $c_0$  and steeper profiles because, as shown by HS by fitting numerically some  $c^{-\alpha}$  profiles to the general formula (63) for given values of  $c_0$ , the smaller  $c_0$ , the steeper is the density profile.

$n$	$\Omega_i$	$c_{0,G}$	$c_{0,E}$	$\alpha_G$	$\alpha_E$
-2	0.7	6.2	2.7	2.2	2.5
	0.8	10.6	4.7	1.9	2.1
	0.9	23.9	10.6	1.7	1.8
	1.0	$\infty$	$\infty$	1.5	1.5
-1	0.7	3.7	2.9	2.8	2.9
	0.8	4.9	3.8	2.5	2.6
	0.9	7.3	5.7	2.2	2.3
	1.0	$\infty$	$\infty$	2.0	2.0

Table 3: The slopes of profiles  $c^{-\alpha}$  fitted in the range  $1 < c < 10$  in the linear (G) and weakly nonlinear (E) case for spectral indices  $n = -2$  and  $n = -1$  and different values of  $\Omega_i$ .

The impact of weak nonlinearity can therefore be seen only at intermediate values of  $c_0$  when the correction to  $c_0$  given by equation (59) is significant. To estimate the correction to the slope introduced by the change in  $c_0$  we perform fits similar to those of HS here first with  $c_0$  given by the linear value (58) and then the weakly nonlinear one, (59). The fits should be treated only as indicative because they are not rigorous perturbatively. We adopt the maximum value of  $a\sigma = 1$  allowed by the Edgeworth approximation and find that the weakly nonlinear  $c_{0,E}$  (for reasonable  $n \geq -2$ ) can be as low as  $c_{0,G}/2$ . The results of the numerical fits of the form  $c^{-\alpha}$  to the formula (63) in the range  $1 < c < 10$  for the values of  $c_0$  corresponding to different values of  $\Omega_i \leq 1$  in the case of  $n = -1$  and  $n = -2$  are given in Table 3.

The results clearly display the dependences on  $\Omega_i$  and  $n$  discussed by HS: profiles are steeper for lower  $\Omega_i$  and higher  $n$ . The weakly nonlinear approximation however predicts steeper slopes for  $\Omega_i < 1$  than the linear approximation does. Only the case of  $\Omega_i = 1$  remains unaffected. Therefore in general weakly nonlinear corrections act in the same directions as decreasing  $\Omega_i$  or increasing  $n$ . This must be taken into account were the slopes of the profiles used to determine these cosmological parameters.

Another important quantity characterizing the protoobject is its mass. We assume that the mass contained initially within radius  $c_0$

$$M(c_0) = \frac{4\pi}{3}(c_0 R)^3 \rho_{b,i}(1 + \Delta_i(c_0)) \quad (66)$$

does not change as the shells collapse and may be treated as the final mass of the protoobject. In this case the quantitative prediction concerning the correction to the mass gathered by the peak can be made. In the linear approximation the mass  $M_G$  is calculated with  $c_{0,G}$  and  $\Delta_{i,G}(c_0)$  given by equations (58) and (52) respectively while in the weakly nonlinear case ( $M_E$ ) they should be replaced by the values given in equations (59) and (53). For the ratio of the masses we obtain

$$\frac{M_E}{M_G} = 1 - 3 \frac{(S_3 - s_{12})(a^2 - 1)}{2(n + 3)a} \sigma. \quad (67)$$

Thus the mass gathered by the peak predicted by weakly nonlinear approximation is always smaller than in the linear case and the correction is larger for lower spectral indices.

## 5 Concluding remarks

The picture emerging from the presented results is the following. In the weakly nonlinear field the average overdensity around the peak, which drives the evolution of matter around it, behaves as if produced by the peak of reduced height embedded in the linear field. Weakly nonlinear interactions decrease the size of region from which the peak gathers mass and the slope of the final density profile is steepened. The type of dependence of the profiles on the cosmological parameters  $\Omega$  and  $n$  derived by HS is preserved.

It should be remembered that the results presented here were obtained for the mean density perturbation,  $\langle\Delta_{i,E}\rangle$ , using the mean normalized density contrast  $\langle\mu\rangle$  calculated from the conditional distribution (38). In order to specify the uncertainty of the results it would be desirable to know also the standard deviation of  $\Delta_{i,E}$ ,  $\sigma_{\Delta}$ , since only below the scale determined by the condition  $\Delta_{i,E} = \sigma_{\Delta}$  the perturbation  $\Delta_{i,E}$  is significant. Such scale would always be finite and dependent on the power spectrum. In the case of  $\Omega_0 = 1$  universe this would mean that we cannot indiscriminately apply the limit  $c_0 \rightarrow \infty$ , which is rather unrealistic: gravitational influence of a peak cannot reach infinite distances because there are always neighbouring peaks that gather mass. Calculating  $\sigma_{\Delta}$  in the weakly nonlinear regime would however require constructing the three-point Edgeworth series, which is beyond the framework of this paper.

There are other limitations to the weakly nonlinear approach to the collapse of peaks presented here. The most obvious one is the condition  $a\sigma < 1$  that must be satisfied for the Edgeworth approximation to be valid. Is the evolution in this regime representative of the fully nonlinear clustering? Another question is how the linear and weakly nonlinear results should be compared. Throughout this paper we assumed the linear value of the variance of the density which is correct as far as we use the lowest order Edgeworth approximation. However, Lokas et al. (1996) have shown that the value of  $\sigma$ , the typical fluctuation of density, itself changes during weakly nonlinear evolution. It remains to be understood how the evolution of a typical fluctuation and evolution of matter around a peak are related.

Observational data concerning the halo density profiles are presently very sparse and derived most often from the fact that the observed rotation curves of galaxies are flat, which in the Einstein-de Sitter universe leads to the profile  $r^{-2}$  that according to formula (64) corresponds to  $n = -1$ . Such spectral index is roughly consistent with what is observed at weakly nonlinear scales but we can hardly go beyond such rough consistency checks as far as observations are concerned. Therefore although such data are of potential cosmological interest the only way to verify the theoretical predictions is to resort to N-body simulations.

The profiles of dark halos have been measured in N-body simulations by many authors including Dekel, Kowitt & Shaham (1981) Quinn, Salmon & Zurek (1986), Efstathiou et al. (1988) and Crone, Evrard & Richstone (1994). The results of such simulations seem to converge to a statement that the present structure of halos retains information on the initial conditions and displays the dependence on cosmological parameters. Crone et al. (1994) performed simulations for power-law spectra and different density parameters  $\Omega_0$  and confirmed the overall trend of steeper density profiles with increasing  $n$  or decreasing  $\Omega$  as predicted by HS. However, the fitted slopes were systematically steeper than those given by HS. As discussed in the previous section only in the case of the open universe such discrepancy can be assigned to the weakly nonlinear effects. The detailed comparison of the predictions of perturbation theory with the results of N-body simulations requires further assumptions (concerning e.g. the epoch of the formation of

objects, the most realistic value of  $a\sigma$  to be adopted) and is currently under way.

Recently Sheth & Jain (1997) proposed a new derivation of the slopes of halo profiles from the shape of nonlinear correlation function based on the assumption that the halo-halo correlations can be neglected i.e. that for sufficiently small scales the input to the correlation function comes mostly from one halo. The slope they obtain,  $\alpha = 3(n + 4)/(n + 5)$ , can be derived within the formalism of HS, and would be obtained instead of the result (64), if the initial profile of the cumulative density is chosen to be  $c_i^{-(n+4)}$  instead of  $c_i^{-(n+3)}$  as in equations (52)-(53). Sheth & Jain (1997) claim that such an initial profile is well motivated by the results of Bardeen et al. (1986) who found that as the peak height decreases the initial profile becomes steeper than  $c_i^{-(n+3)}$ . In this case the approximation used here (i.e. regions of high enough density, and not necessarily peaks, are the progenitors of structure) would be less accurate.

This objection can only be valid under condition that smaller peaks can collapse by themselves to form objects. N-body simulations performed by Katz, Quinn & Gelb (1993) and van de Weygaert & Babul (1994) suggest the opposite: there is no clear correspondence between peaks in the initial density field and the actual halos for smaller peaks. For example, Katz et al. (1993) find that most of the peaks expected to form cluster-size objects ( $a \geq 4$ ) indeed end up in such objects while the peaks from which the galaxy-size objects form ( $a \approx 2$ ) may end up in a galaxy-size group as well as merge with a larger object. Even more possibilities for the history of a peak, including its breaking into few distinct halos, were found by van de Weygaert & Babul (1994).

## Acknowledgements

I wish to thank Roman Juszkiewicz for suggesting to me the investigation of the two-point Edgeworth series. I am also grateful to Michał Chodorowski and François Bouchet for their comments at different stages of this work. The hospitality of the Institut d'Astrophysique de Paris, where part of this work was done, is kindly acknowledged. This work was supported in part by the Polish State Committee for Scientific Research grants No. 2P30401607, 2P03D00310 and 2P03D01313, and the French Ministry of Research and Technology within the programme Jumelage (Astronomie Pologne).

## References

- Adler, R. J. 1981, "The Geometry of Random Fields" (Chichester: Wiley)
- Bardeen, J. M., Bond, J. R., Kaiser, N. & Szalay, A. S. 1986, *ApJ*, 304, 15
- Bernardeau, F. 1994, *ApJ*, 433, 1
- Bernardeau, F. 1996, *A&A*, 312, 11
- Bernardeau, F. & Kofman, L. 1995, *ApJ*, 443, 479
- Crone, M. M., Evrard, A. E. & Richstone, D. O. 1994, *ApJ*, 434, 402
- Dekel, A. 1981, *A&A*, 101, 79
- Dekel, A., Kowitt, M. & Shaham, J. 1981, *ApJ*, 250, 561
- Efstathiou, G., Frenk, C. S., White, S. D. M. & Davis, M. 1988, *MNRAS*, 235, 715
- Gott, J. R. 1975, *ApJ*, 201, 296
- Gunn, J. E. 1977, *ApJ*, 218, 592
- Gunn, J. E. & Gott, J. R. 1972, *ApJ*, 176, 1
- Hoffman, Y. & Shaham, J. 1985, *ApJ*, 297, 16 (HS)
- Juszkiewicz, R., Bouchet, F. R. & Colombi, S. 1993, *ApJL*, 412, L9
- Juszkiewicz, R., Weinberg, D. H., Amsterdamski, P., Chodorowski, M. & Bouchet, F. R. 1995, *ApJ*, 442, 39
- Katz, N., Quinn, T. & Gelb, J. M. 1993, *MNRAS*, 265, 689
- Lokas, E. L., Juszkiewicz, R., Weinberg, D. H. & Bouchet, F. R. 1995, *MNRAS*, 274, 730
- Lokas, E. L., Juszkiewicz, R., Bouchet, F. R. & Hivon, E. 1996, *ApJ*, 467, 1
- Longuet-Higgins, M. S. 1963, *Journal of Fluid Mechanics*, 17, 459
- Longuet-Higgins, M. S. 1964, *Radio Science Journal of Research*, 68D, 1049
- Peebles, P. J. E. 1980, "The Large-scale Structure of the Universe" (Princeton: Princeton University Press)
- Peebles, P. J. E. 1984, *ApJ*, 277, 470
- Quinn, P. J., Salmon, J. K. & Zurek, W. H. 1986, *Nature*, 322, 329
- Sheth, R. K. & Jain, B. 1997, *MNRAS*, 285, 231
- van de Weygaert, R. & Babul, A. 1994, *ApJ*, 425, L59